

Investigations into the Cylinder Flow Stabilities with a Thin Film Attachment

Deog-Hee Doh[†] · Hyo-Je Jo¹ · Seang-Yong Kwon² · Hyoung-June Kim² · Gyeong-Rae Cho³ · Byeong-Rog Shin⁴

(Received November 16, 2011; Revised November 28, 2011; Accepted November 28, 2011)

Abstract : The wakes of a cylindrical body have been investigated. The cylindrical body was attached with a thin film. The film is made of silicon with configurations of 50mm(W) x 150mm(L) x 0.3mm(T). The cylinder wakes have been measured with PIV experiments under the conditions with and without the thin film. The diameter of the installed cylinder body is 30mm and the Reynolds numbers are 2730, 6160 and 9750 with the diameter. The measurement system consists of an Ar-ion laser(6W), a high speed camera(1024 x 992 pixel, 500fps) and a host computer. FFT analyses have been carried out using the velocity vectors obtained by PIV measurements at the point $X/D=1.52$ and $Z/D=0.52$. For understanding the three-dimensional flow structures, a new Volumetric PTV(particle tracking velocimetry) has been constructed, in which the same four high-resolution cameras have been used. It has been verified that the flexible film suppresses or damps the vortices separated from the cylinder body, which makes the cylinder's wakes stable. With increase of Re numbers the intensity of the dominant frequency of the wakes become smaller.

Key words : Stabilization, Cylinder Wake, Thin Film, 2D-PIV, Volumetric PTV

1. Introduction

The VIV(vortex induced vibration) affects the dynamics of riser tubes bringing oil from the seabed to the surface, as well as civil engineering structures such as bridges, chimneys, and buildings, further for offshore and ocean structures' applications. The range of problems caused by vortex- induced vibration has led to a large number of experimental and computational studies on the subject, including several review articles [1, 2, 3, 4, 5]

In studies of vortex-induced vibration, the case of an elastically mounted rigid cylinder, constrained to move transverse to an incoming flow, is often used as a paradigm for understanding more diverse

experimental arrangements [6]. Williamson and Roshko [7] studied the vortex wake patterns for a cylinder, forced to translate in a sinusoidal trajectory, over a wide variation of amplitudes (A/D up to 5.0) and wavelengths (l/D up to 15.0). They defined a whole set of different regimes for vortex wake modes, in the plane of $\{l/D, A/D\}$, where a descriptive terminology for each mode was introduced. Each periodic vortex wake pattern comprises single vortices (S) and vortex pairs (P), giving patterns such as the 2S, 2P and P+S modes.

Donald Rockwell's group at Lehigh University [8] were the first to measure vorticity dynamics using PIV on the problem of controlled cylinder vibration. The first

[†] Corresponding Author(Div. of Mech. & Energy Systems Eng., Korea Maritime Univ., E-mail:doh@hhu.ac.kr, Tel:051-410-4364)

1 Div. of Naval Arch. & Ocean Systems Eng., Korea Maritime Univ.

2 Dept. of Refrigeration and Air-conditioning Eng., Graduate School, Korea Maritime Univ.

3 Research Inst. of Ocean Science and Tech., Korea Maritime Univ.

4 Dept. of Mech. Eng., Changwon National Univ.

This paper is extended and updated from the short version that appeared in the Proceedings of the International symposium on Marine Engineering and Technology (ISMT 2011), held at BEXCO, Busan, Korea on October 25-28, 2011.

vorticity measurements for free vibrations, by Govardhan and Williamson [9], confirmed that the initial and lower branches correspond to the 2S and 2P vortex wake modes respectively.

In the mean while, there are several studies in controlling the wake behind a circular cylinder. Fujisawa [10] used a small cylinder for controlling the wake of the main cylinder. Sakamoto et. al [11] used a fine flat film to suppress of the forces acting on the cylinder. Fuchiwaki et al. [12] used an elastic airfoil to control the wake generated its behind. Gomes and Lienhart [13] carried out an experiment using PIV technique to check the fluid-structure interaction problems on the cylinder wake behind which a thin film was attached. Their measurements were carried out using two-dimensional PIV.

In this study, the control characteristics of a thin film which is attached behind a circular cylinder are investigated using a 2D-PIV and a Volume PTV.

2. Experiments

Figure 1 shows the overall experimental setup. A cylinder ($D=30\text{mm}$) is installed inside of the circulating water channel ($1100\text{mm} \times 300\text{mm} \times 300\text{mm}$). A thin film (silicon) of which size it $0.3\text{t} \times 500\text{mm} \times 150\text{mm}$ has been attached onto the body of the cylinder as shown in Figure 1. The tested Reynolds numbers are 2730, 6160 and 9750. In order to investigate the flow characteristics of the flow, a PIV system has been used. The system consists of an Ar-ion laser (5W, continuous) for visualizations of the flow field, a high speed camera (1024 x 992 pixel, 500fps) and a host computer. FFT analysis has been carried out using the measured velocity vectors obtained by PIV. The sampling position for the acquisition of the velocity vector is at $X=1.52D$ and $Y=-0.52D$ from the center position of the system as shown in Figure 2.

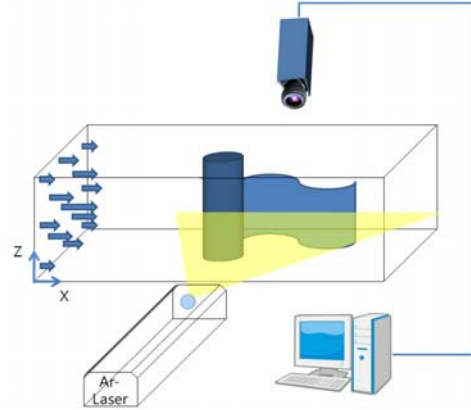


Figure 1: Experimental setup.

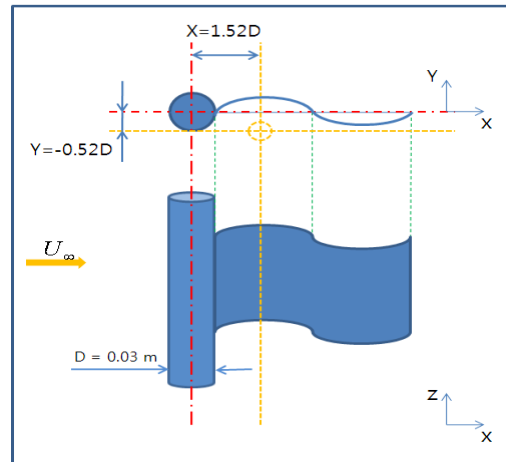


Figure 2: Coordinate relations for vector sampling.

2.1 FFT analyses with 2D-PIV Measurements

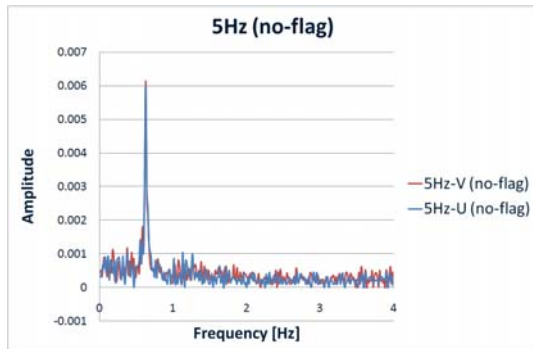
Table 1: Comparison with frequency f and f_{exp} .

Re_D	St	f $u_{\infty} (=St*/D)$	f_{exD} (no-flag)	f_{exD} (flag)
2730	0.21	0.6	0.63	0.64
6160	0.204	1.4	1.45	1.87
9750	0.199	2.2	2.22	2.18

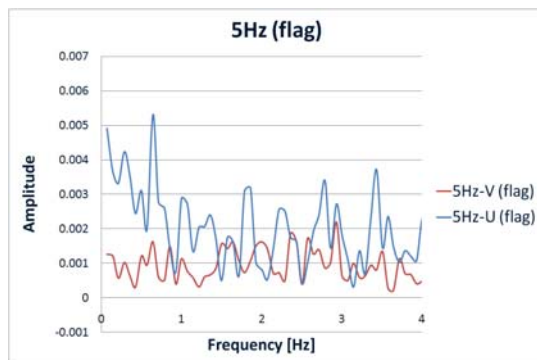
Table 1 shows the comparison results on the frequencies measured by Rousan and Wu[14], Williamson[15] and Rey[16] with our experimental results. The frequency f in the table has been calculated from the Re_D and St in their reports. f_{exp}

shows the frequency obtained in this experiment. Here, ‘no-flag’ means that the thin film has not been attached and ‘flag’ means the contrary. It can be seen that there is no significant difference in f values except at the Reynolds number $Re_D=6160$ when the thin film has been attached. This implies that the shedding frequency of vortex at this condition is being controlled by the thin film.

Figure 3 shows the FFT results at $Re_D=2730$ when the thin film is not attached (no-flag) and the attached (flag). The U-components at the case of having the flag show different profiles from those at the case of without the flag. That is, there is no significant frequency in V-component when the flag has been attached.

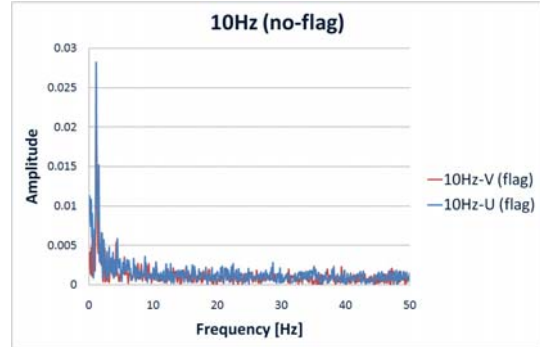


(a) without the thin film

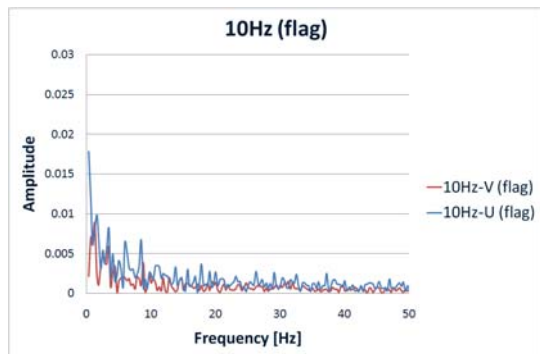


(b) with the thin film

Figure 3: FFT analysis results on the PIV data at $Re_D=2730$.



(a) without the thin film



(b) with the thin film

Figure 4: FFT analysis results on the PIV data at $Re_D=6160$.

This means that the flag controls the vortices at the downstream of the wake. Further, the frequency of the u-components shows smooth profiles. This implies that the flag plays a role of suppressing the high frequencies of the vortices.

Figure 4 shows the FFT results at $Re_D=6160$ for the two cases without the flag and with the flag, too. There is no significant difference in V-components between the two cases. But, the amplitude of the U-component in the case of having flag has been significantly reduced than the case of no-flag. On top of it, the frequency itself has been increased higher than in the case of no-flag. This implies that the flag plays a significant role in controlling the vortices shed from

the cylinder at this $Re_D=6160$. The fact that the dominant frequency at the case of having the flag has been shifted to higher one indicates that the vortices generated behind the cylinder would have been broken due to the flag's motion. This phenomenon can be explained by Figure 5. In Figure 5, the red colored point show the location of data sampling. This figures show that the flag's state

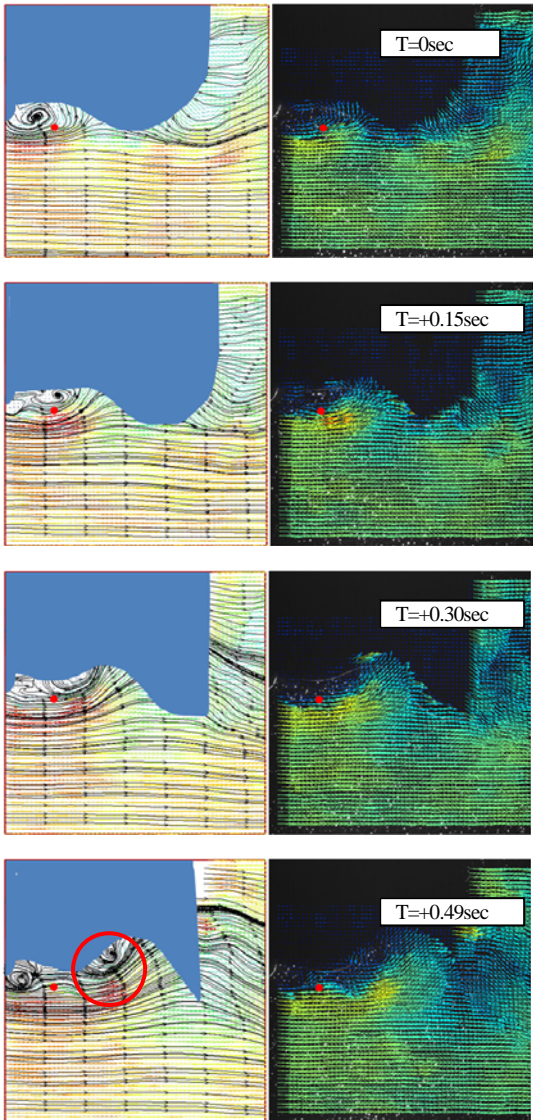
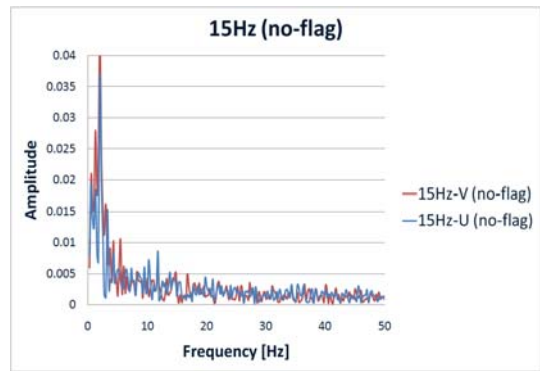


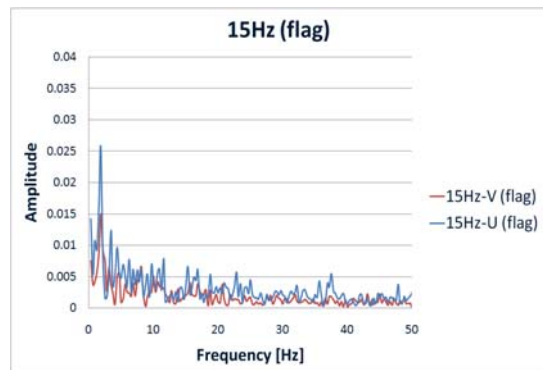
Figure 5: Instantaneous vector fields with the thin film.

and the flow around it. With time increasing, the flag is going downward toward the red point. This means that the curved flag plays as an obstacle against the vortices coming from upstream, and eventually these vortices become broken due to this convex surface(see at $T=+0.49\text{sec}$ in Figure 6, circle area).

Figure 6 shows the FFT results at $Re_D=9750$ for the two cases. The amplitude of V-component in the case of having flag has been largely reduced than in the case of no-flag. The amplitude of U-component has been also reduced than that of the case in no-flag. However, there is no difference in the dominant frequencies between the two cases.



(a) without the thin film



(b) with the thin film

Figure 6: FFT analysis results on the PIV data at $Re_D=9750$.

2.2 Investigation of Flow structures with Volumetric PTV Measurements

In order to investigate the role of vortices in three-dimensional, a new volumetric measurement technique has been constructed. Figure 7 shows an experimental setup for this. Four cameras (1024 x 992 pixel, 500fps) were used for capturing instantaneous flow motions. Small particles (d=0.1mm) were used as tracers for PTV (particle tracking velocimetry). The Reynolds number for this test is 4800. For flow visualizations, the same Ar-ion laser (5W, continuous) used in the 2D-PIV in the previous section was used. Since image data from the four cameras are quite big, two host computers were used, and they were synchronized by a house made control system. In order to get the three-dimensional motion of those particle seeded in the channel, 3D-PTV algorithm[17] developed by the author has been revised. Generally, a process called ‘camera calibration’ should be carried out for the four cameras in advance before using them as the sensors for image capturing. Detailed calibration method is well explained in the reference[17].

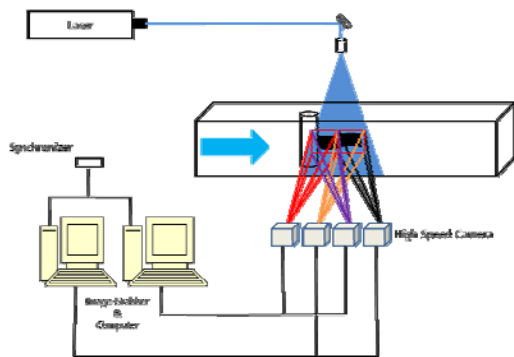


Figure 7: Experimental setup for Volumetric PTV measurements.

2.2.1 Measurement Principle

Figure 8 shows the overall tracking procedure of the Volumetric PTV. Vector tracking algorithm is made as follows. (1) Obtain the 2-dimensional vectors for each camera within a certain displacement.

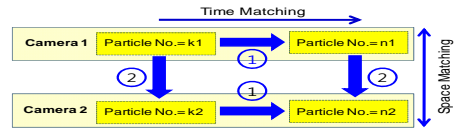


Figure 8: Overall procedure for vector acquisitions.

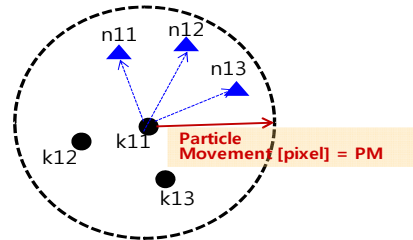


Figure 9: Definition of particle movement [PM].

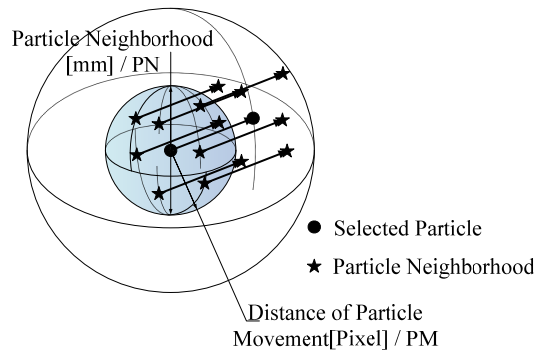


Figure 10: Definition of particle neighbourhood [PN].

Here, PM (particle movement) has been set to a certain pixel value according to the flow speed. This procedure is called as time matching. (2) Find candidate of particle pairs on the image of camera 2. Here, Epipolar line has been used to find the candidate particles on the image of the camera 2 and to save calculation time. For the particle 'n1' and 'n2', the same procedure for finding the candidates is made. Once the candidate (k2) of the particle image of the camera 2 for the initial point (k1) are found, the terminal point of

the 2D vector is automatically decided since the 2D vectors had been already obtained. If the candidate for particle 'n1' is found within the Epipolar search area, the particle set of (k1, n1, k2, n2) is sorted into the candidate group. (3) For the whole particles in the images of the camera 1 and the camera 2(Figure 9), the candidate group database is constructed. (4) For the candidate group database, a particle neighborhood value [PN] is set to a certain value [mm]. Within this PN (Figure 10), a vector fitness [VF] is calculated using Eq. (1). u_i indicates the whole vectors within PN except the target vector itself and u_o represents the mean value of the whole vectors within PN except the target vector itself. (5) Lastly, a sigmoid-like hybrid fitness function (Figure 11) defined as equation Eq. (2) is used for sorting out the most probable candidate from the candidate group database. Using PN and PM values implies to find a coherency of the neighborhood particles. It has been shown that the optimal parameters are PM=8 pixel, PN=5mm and VF=0.3. More detailed explanation for the measurement algorithm is to be referred to the paper done by Doh et al. [18]. For the camera calibration for three-dimensional reconstruction is to be referred to the reference [17].

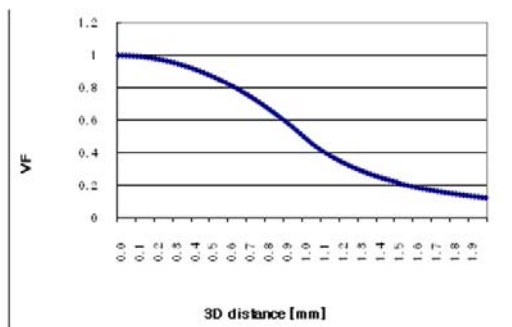


Figure 11: Hybrid fitness function used for sorting the most probable candidate from the candidate group database.

$$Vector\ Fitness[VF]=\frac{\sum |u_i - u_o|}{\sum u_i} \tag{1}$$

$$f(x) = \begin{cases} -0.5x^2 + 1, & \text{at } (0 \leq x \leq 1) \\ 0.5x^{-2}, & \text{at } (x \geq 1) \end{cases} \tag{2}$$

2.2.2 Measurement Results

Figure 12 shows the measurement volume behind the cylinder wake. The front volume has been measured by the first camera and the third camera from the left in Figure 7. And the rear volume has been measured by the second camera and the fourth camera. The whole volume size is 150mm(L) x 60mm(H) x 15mm(T).

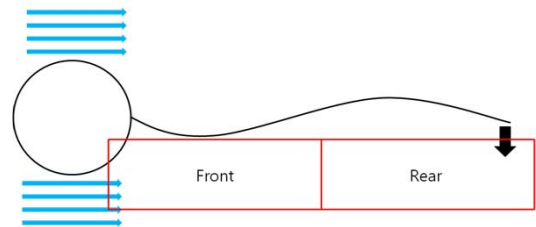


Figure 12: Measurement volume for the Volumetric PTV.

Figure 13(a) shows instantaneous velocity vector distribution in volume at time T=T1 and Figure 13(b) shows the one at T=T2. The time difference between the two results is 1/200sec. In Figure 13(a), there is a strong local vortex at the region (see the ellipse colored blue) at the boundary between the front and the rear volumes. But, this vortical structures at the time T=T1 + 1/200 [sec] spread over the whole spanwise direction. This implies that the thin film controls the vortices shed from the cylinder widely over the whole region. This might have been occurred by the vortices' merging or breaking. Figure 14 (a) and Figure 14 (b) show the spatial distributions of the three-dimensional velocity vector at five cross sections along the spanwise. Clearly, the local vortical structures at

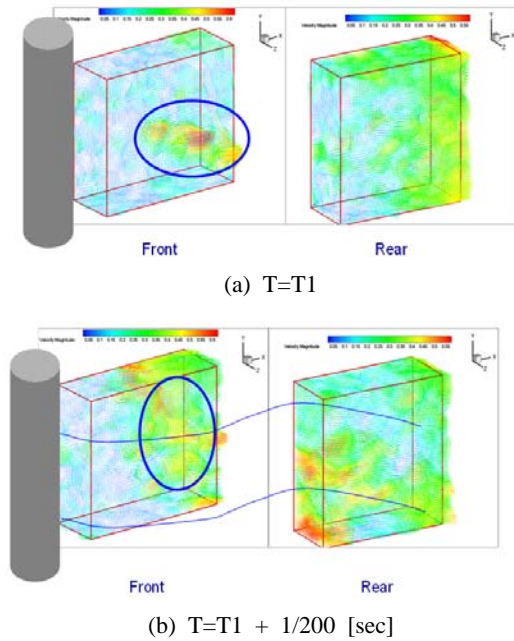


Figure 13: Volumetric velocity vector distribution obtained by the Volumetric PTV.

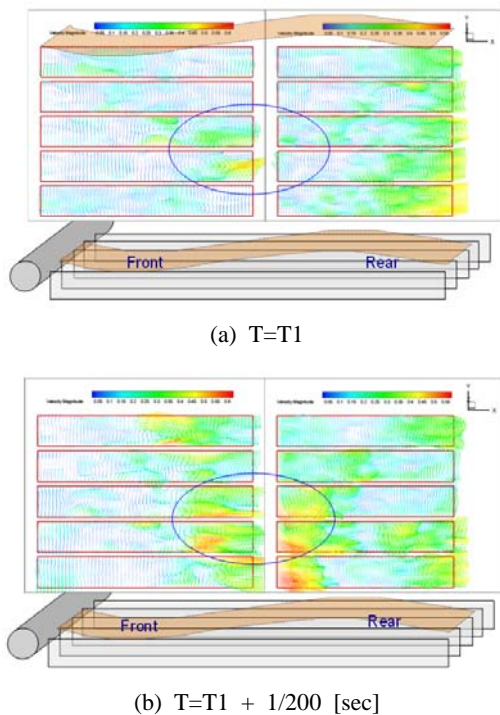


Figure 14: Cross sectional distribution of the three-dimensional velocity vectors of Figure 13.

time $T1$ are seen at the center section, while these structures become spread over the whole spanwise region. This implies that the momentum affecting the cylinder is controlled by these vortices, eventually implying the cylinder's stabilizations.

3. Conclusions

The purpose of the study is to investigate the role of vortices controlled by a thin film which has been attached to the rear part of a circular cylinder. To do this, two measurements have been carried out, one with 2D-PIV system and the other one with a newly constructed volumetric PTV system. Followings are several key results from the experiments.

There are big changes in U-component when the flag has been attached to the cylinder. The amplitudes of U-component were always reduced at all Reynolds numbers, and the reduction degree of the amplitude of U-component at $Re_D=6160$ was larger than any other cases. Further, the dominant frequency at $Re_D=6160$ became increased while those at other Reynolds numbers showed no changes with that in the case of no-flag.

Especially, U-component at $Re_D=2730$ became smoothed, which can not be seen at other Reynolds numbers. This implies that the vortices behind the cylinder at this Reynolds number become merged. On the contrary, the most dominant frequency of U-component at $Re_D=6160$ with the flag became shifted to a higher frequency region. This implies that the vortices shed from the cylinder become broken state but not the merging state at $Re_D=2730$.

For V-components, the frequency at $Re_D=2730$ became smoothed while other two cases were not. And the amplitude of V-component $Re_D=6160$ and $Re_D=9750$ became largely suppressed by the flag, which implies that a possible oscillation made by the vortices around the cylinder become reduced or

stable. This implies that the thin film plays a role of stabilizations for the cylinder.

Acknowledgments

This work was supported by the National Research Foundation of Korea (NRF) grant funded by the Korea government (MEST) (No. 2008-0060153), and was partly supported by Manpower Development Program for Marine Energy by Ministry of Land, Transport and Maritime Affairs(MLTM).

References

- [1] P.W. Bearman, "Vortex shedding from oscillating bluff bodies", *Annual Review of Fluid Mechanics*, vol. 16, pp. 195-222, 1984.
- [2] G. Parkinson, "Phenomena and modeling of flow-Induced vibrations of bluff bodies. *Progress in Aerospace Sciences*", vol. 26, pp. 169-224, 1989.
- [3] T. Sarpkaya, "Hydrodynamic damping, flow-induced oscillations, and biharmonic response", *ASME Journal of Offshore Mechanics and Arctic Engineering*, vol. 117, pp. 232-238, 1989.
- [4] C.H.K. Williamson and R. Govardhan, "Vortex-induced vibrations". *Annual Review of Fluid Mechanics*, vol. 36, pp. 413-455, 2004.
- [5] C.H.K. Williamson and R. Govardhan, "A brief review of recent results in vortex-induced vibrations", *Journal of Wind Engineering and Industrial Aerodynamics*, vol. 96, pp. 713-735, 2008.
- [6] T.L. Morse, and C.H.K. Williamson, "Employing controlled vibrations to predict fluid forces on a cylinder undergoing vortex-induced vibration", *Journal of Fluids and Structures*, vol. 22, pp.877-884, 2006.
- [7] C.H.K. Williamson and A. Roshko, "Vortex formation in the wake of an oscillating cylinder", *J. Fluids Struct*, vol. 2, pp. 355-381, 1988.
- [8] W. Gu, C. Chyu and D. Rockwell, "Timing of Vortex Formation from an Oscillating Cylinder", *Phys. Fluids*, vol. 6, pp. 3677-3682, 1994.
- [9] R. Govardhan and C.H.K. Williamson, "Modes of vortex formation and frequency response for a freely vibrating cylinder", *J. Fluid Mech.*, vol. 420, pp.85-130, 2000.
- [10] N. Fujisawa and H.M. Warui, "Active control of vortex shedding from circular cylinder by cross-flow cylinder oscillations", *JSME(C)*, vol. 65, no. 585, pp. 1827-1831, 1995.
- [11] H. Kakamoto, H. Haniu, S. Matubara and Y. Obata, "Optimum suppression of fluid forces acting on a circular cylinder and its Effectiveness-controlled by a Fine Flat Plate", *JSME(B)*, vol. 58, no. 548, pp. 1079-1085, 1992.
- [12] M. Fuchiwaki, T. Kurinami, and K. Tanaka, "Detailed wake structure behind an elastic airfoil", *Journal of Fluid Science and Tech.*, vol. 4, no. 2, pp. 391-400, 2009.
- [13] J.P. Gomes and L. Hermann, Time-phase Resolved PIV/DPI Measurements on Two-dimensional Fluid-Structure Interaction Problems, the 13th Int. Symp. on Applications of Laser Tech. to Fluid Mechanics, Lisbon, Portugal, 26-29 June, Paper No.1102, 2006.
- [14] P. Roushan and X.L. Wu, Structure-Based Interpretation of the Strouhal-Reynolds Number Relationship, *Phys. Rev. Lett.*, Vol. 94, 054504-3-054504-7, 2005.
- [15] H.K. Williamson, "A series in to represent the strouhal-reynolds number relationship of the cylinder wake", *Journal of Fluids and Structures*, vol. 12, pp. 1076-1081, 1998.
- [16] U. F.M. Konig, and H. Eckelmann, "A new strouhal-reynolds-number relationship for the

circular cylinder in the Range $47 < Re < 2 \times 10^5$ ", Phys. Fluids, vol. 10, no. 7, pp. 1547-1549, 1998.

- [17] D.H. Doh, D.H. Kim, K.R. Cho, Y.B. Cho, T. Saga and T. Kobayashi, "Development of GA based 3D-PTV Technique", Journal of Visualization, vol. 5, no. 3, pp. 243-254, 2002.
- [18] D.H. Doh, H.J. Jo, G.R. Cho, J.M. Lee, K.R. Moon, and M. Takei, "Investigations of Flow Structures and Turbulent Properties of Cylinder Wakes by a Volume PTV", the 8th International Symp. on PIV, Melbourne, Victoria, Australia, August 25-28, 2009.



Hyoung-June Kim

He received his B.S. degree in Refrigeration and Air conditioning and Energy Systems from Korea Maritime Univ. in 2010 and He will finish his M.S. degree at KMU in 2012.



Gyeong-Rae Jo

He received his B.S. degree in Refrigeration and Air conditioning and Energy Systems from Korea Maritime Univ. in 1999. He then received the Ph.D. degree in Mechanical Eng. in Saitama Univ. in 2004.



Byeong-Rog Shin

He received his Ph.D. degree in Mechanical Eng. from Tohoku Univ., Japan, in 1991. He is currently a professor in the Dept. of Mechanical Eng., Changwon National Univ., Korea. His research interests are in the areas of fluid mechanics and CFD to clarify flow phenomena, as well as in the areas of the numerical scheme and simulation for the prediction, optimal design and the improvement of the performance of turbomachinery systems.

Author Profile



Deog-Hee Doh

He received his B.S. and M.S. degrees in the dept. of Marine Eng. in Korea Maritime Univ.(KMU) in 1985 and 1988, respectively. He received his Ph.D. degree in the Dept. of Mech. Eng. in Tokyo Univ., Japan, in 1995. He is currently a professor in the Div. of Mech. and Energy Systems Eng. at KMU. Main interests are in the areas of Flow Visualizations in Industry and Marine and Offshore Machinery.



Hyo-Je Jo

He received his B.S. and M.S. degrees in the Dept. of Naval Architecture and Shipbuilding in 1980 and 1983, respectively. In 1991, he received his Ph.D. degree in the Dept. of Ship and Ocean Eng. of Tokyo University in 1991. He is currently a professor in the Div. of Naval Architecture and Ocean Systems Eng. in KMU.



Seong-Yong Kwon

He received his B.S. degree in Refrigeration and Air conditioning and Energy Systems from Korea Maritime Univ. in 2010 and He will finish his M.S. degree at KMU in 2012.